A Trade-Off Function $a_0(\beta)$

Figure A.1 shows how the trade-off function defined by equation (4) in the main text varies with transmission coefficient β for different values of c.

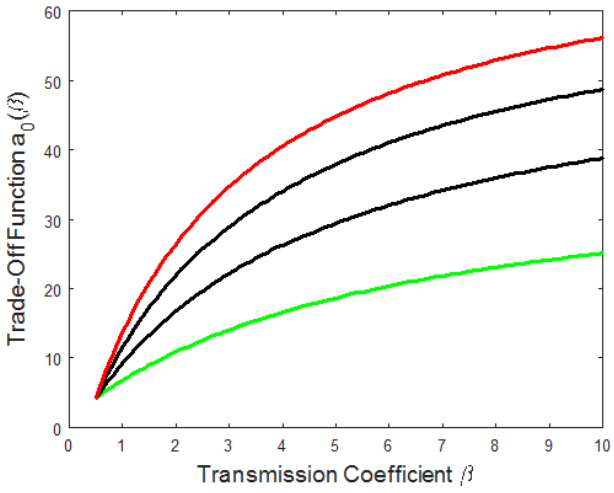

Figure A.1: Trade-off function $a_0(\beta)$ as defined in equation (4) of the main text for varying transmission coefficient β and different values of c increasing from 1.5 (green) to 3 (red) in steps with size 0.5. Default parameters were otherwise used.

B How To Find The Host Fitness When $\gamma > 0$

The adaptive dynamics method involves adding a rare mutant with susceptible and infected population sizes S_m, I_m and transmission coefficient β_m very close to the resident transmission coefficient β. Assumptions for this method are outlined in the main text. We therefore have equations for the mutant population:

$$\frac{dS_\mathrm{m}}{dt} = a_0(\beta_\mathrm{m})(1+\delta\sin(2\pi t/\epsilon))(1-q(N+N_\mathrm{m}))S_\mathrm{m} - bS_\mathrm{m} - \beta_\mathrm{m}S_\mathrm{m}(I+I_\mathrm{m}) + \gamma I_\mathrm{m}, \tag{B.1}$$

$$\frac{dI_\mathrm{m}}{dt} = \beta_\mathrm{m}S_\mathrm{m}(I+I_\mathrm{m}) - (b+\alpha+\gamma)I_\mathrm{m}, \tag{B.2}$$

where $N_\mathrm{m} = S_\mathrm{m} + I_\mathrm{m}$ is the total mutant population, and $S = S(t)$, $I = I(t)$ are the resident dynamics from the equations in the main text evaluated on the limit cycle found before a mutant is introduced.

Equations (B.1) and (B.2) are easily linearised using the assumption that the mutant is initially rare. To analyse how the host evolves, we consider the mutant's fitness, defined to be the long-term exponential growth rate of the mutant in the current environment (Metz et al., 1992). For $\gamma > 0$, the mutant's fitness is the largest Lyapunov exponent.

To find the Lyapunov exponent, suppose that we have a fundamental solution $\mathbf{X}(t) = (S_{\mathrm{m}}(t)\, I_{\mathrm{m}}(t))$ of the linearised mutant equations (B.1), (B.2) (Grimshaw, 1990). We can then rewrite the problem as:

$$\frac{d\mathbf{X}(t)}{dt} = \mathbf{A}(t)\mathbf{X}(t) \tag{B.3}$$

where $\mathbf{A}(t)$ is a 2 x 2 matrix containing the periodic coefficients. The solution $\mathbf{X}(t)$ is unlikely to be periodic, but we can write the linearly independent solutions to (B.3) in the form $\mathbf{X}_i(t) = e^{\mu_i t}\mathbf{p}_i(t)$ for $i \in \{1, 2\}$, where the $\mathbf{p}_i$ are periodic with period T. From Grimshaw (1990), we can write:

$$\mathbf{X}(t+T) = \mathbf{X}(t)\mathbf{C} \quad \forall\ t \geq 0, \tag{B.4}$$

where $\mathbf{C}$ is a non-singular constant 2 x 2 matrix. We now know that the mutant population grows or decays depending on the signs of the μ_i, which are related to the eigenvalues of $\mathbf{C}$ by $\rho_i = e^{\mu_i T}$. The mutant fitness is therefore the largest of the μ_i: if they are both negative, the mutant dies out; if at least one is positive, the mutant grows.

We are predominantly interested in the sign of the fitness, i.e. whether or not $\max\{\mu_1, \mu_2\}$ is greater or less than zero. This is equivalent to considering whether or not the maximum of the eigenvalues ρ_i is greater or less than 1. Therefore the fitness for our seasonal system is the largest eigenvalue of $\mathbf{C}$ minus 1.

We cannot find the eigenvalues of $\mathbf{C}$ analytically because we cannot solve the mutant equations analytically (Klausmeier, 2008). However, we can find $\mathbf{C}$ numerically by setting $t = 0$ in (B.4), then choosing two linearly independent initial conditions $\mathbf{X}(0)$. By running the mutant equations within the current resident dynamics, this then gives us four equations for the elements of $\mathbf{C}$ in the numerically found components of $\mathbf{X}(T)$. The simplest initial conditions to implement are $(1\,0)$ and $(0\,1)$, which are what we use for this work. The fitness can then be found using this numerically

acquired $\mathbf{C}$.

Note that since $\mathbf{C}$ is a non-negative matrix, the Perron-Frobenius theorem applies and the largest eigenvalue ρ of $\mathbf{C}$ is non-negative. For some positive integer k, we can set $t = t' + (k-1)T$ in equation (B.4) to obtain:

$$\mathbf{X}(t' + kT) = \mathbf{X}(t')\mathbf{C}^k \quad \forall\ t' \geq 0. \tag{B.5}$$

By setting $t' = 0$, we can find the elements of $\mathbf{C}^k$ numerically by running the mutant dynamics up to time kT. From linear algebra results, we know that the eigenvalues of $\mathbf{C}^k$ are ρ_i^k. The fitnesses $(\rho - 1)$ and $(\rho^k - 1)$ obtained from equations (B.4) and (B.5) respectively are of the same sign when ρ is non-negative, hence we find the correct sign for the fitness when the mutant dynamics are run up to time kT for some positive integer k.

C Method for Finding the Population Averages

Let T be the period of oscillation of the hosts (note that this is some integer multiple of ϵ), so we have $S(t+T) = S(t)$ etc. We can take the average of $\frac{dS(t)}{dt}$ and $\frac{dI(t)}{dt}$ over this period to find:

$$\frac{1}{T}\int_{P_0}^{P_1} \frac{dS}{dt} dt = [S(t)]_{P_0}^{P_1} = 0\,, \tag{C.1}$$

and

$$\frac{1}{T}\int_{P_0}^{P_1} \frac{dI}{dt} dt = [I(t)]_{P_0}^{P_1} = 0\,, \tag{C.2}$$

where $P_1 = P_0 + T$ for some arbitrary time $P_0 > 0$ after the population has reached a dynamic attractor. We also have:

$$\frac{1}{T}\int_{P_0}^{P_1} \frac{1}{S}\frac{dS}{dt} dt = [\ln(S(t))]_{P_0}^{P_1} = 0\,. \tag{C.3}$$

and

$$\frac{1}{T}\int_{P_0}^{P_1} \frac{1}{I}\frac{dI}{dt} dt = [\ln(I(t))]_{P_0}^{P_1} = 0\,. \tag{C.4}$$

By using equation (C.4) and the model equation for $\frac{dI(t)}{dt}$, we find with some rearranging that:

$$\hat{S} = \frac{1}{T}\int_{P_0}^{P_1} S(t)dt = \frac{\alpha + b + \gamma}{\beta}\,. \tag{C.5}$$

Using equation (C.2) and the model equation for $\frac{dI(t)}{dt}$, we find that:

$$\hat{I} = \frac{\beta}{(\alpha + b + \gamma)}\frac{1}{T}\int_{P_0}^{P_1} S(t)I(t)dt\,. \tag{C.6}$$

From equations (C.1) and (C.6), we can find an alternative form for $\hat{I}$:

$$\hat{I} = \frac{1}{(\alpha + b)}\left[\frac{1}{T}\int_{P_0}^{P_1}\left\{a(t)S(t)(1 - qN(t))\right\}dt - b\hat{S}\right]\,. \tag{C.7}$$

D Simulation Example

Throughout this paper we confirmed the evolutionary behaviour near the singular points found using PIPs and simulations. Figure D.1 shows an example of a bistability case similar to that examined in the main text. The PIP shows that three singular points exist, specifically 2 CSSs ($\beta^*_{\mathrm{L}} = 3.0941$ & $\beta^*_{\mathrm{H}} = 7.3764$) separated by a repeller ($\beta^*_{\mathrm{R}} = 5.3511$). Simulations confirm the types seen in the PIP, with the host evolving towards β^*_{L} for initial transmission coefficient $\beta_0 < \beta^*_{\mathrm{R}}$ (figures (b) & (c)) and towards β^*_{H} for $\beta_0 > \beta^*_{\mathrm{R}}$ (figures (d) & (e)). This example also demonstrates that the approximation method used to find the fitness is somewhat robust, since in the simulations we have relaxed the assumptions that the resident is monomorphic and that mutations are very small.

E Stability of Solutions for $\gamma = 0$

In figure 1(c) in the main text, we claimed that the discrete change in singular point β^* is due to a change in attractor in the population dynamics. Figure E.1 shows the stability of the 1- and 2-year solutions. We found that for varying amplitude δ, the 1-year solution (black) remains stable up to $\delta = 0.63$, at which point it undergoes a period-doubling bifurcation (and the 1-year solution is then

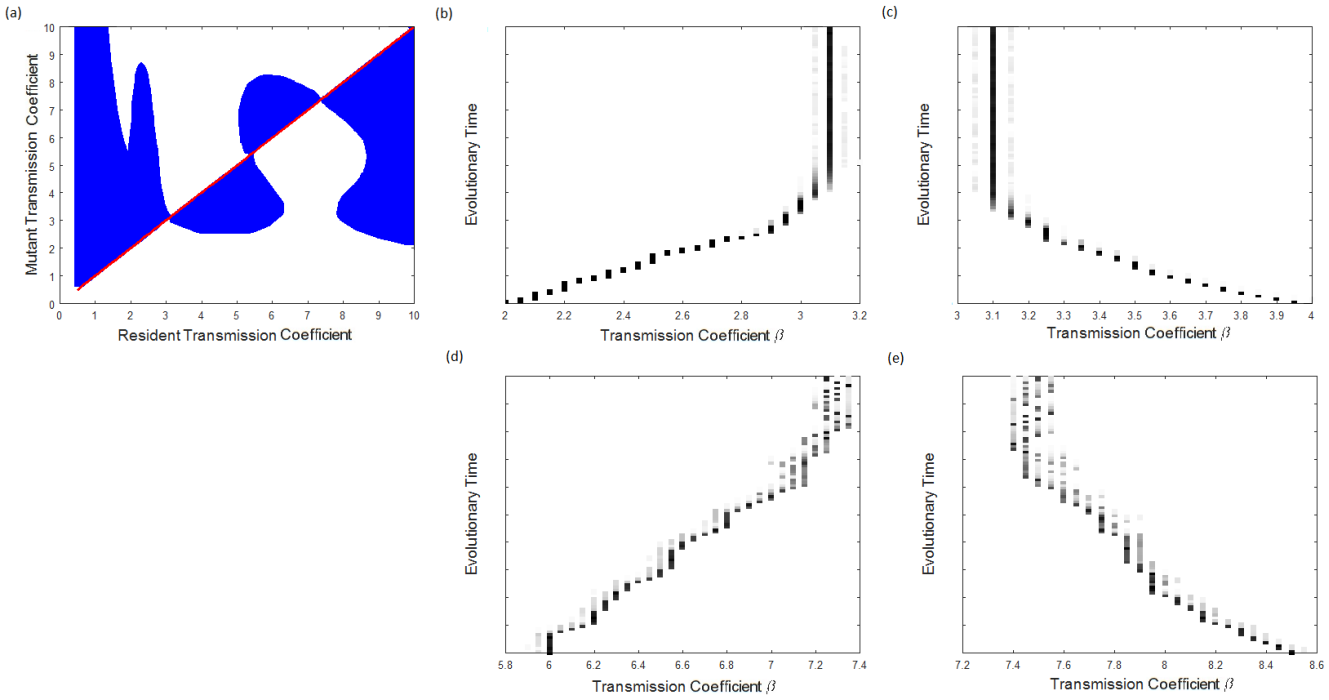

Figure D.1: (a) Pairwise-invasion plot, where blue indicates positive mutant fitness, and the red line is $\beta = \beta_{\mathrm{m}}$. (b),(c),(d),(e) Simulations of the evolutionary behaviour for initial resident transmission coefficient (b) $\beta_0 = 2$, (c) $\beta_0 = 4$, (d) $\beta_0 = 6$ & (e) $\beta_0 = 8.5$. Darker squares indicate a higher proportion of the population with the corresponding transmission coefficient β. Parameters were set at default values except $\hat{a_0} = 104$, $\gamma = 0.03$ & $\delta = 0.75$.

unstable). The red curve that emerges is the 2-year solution. This is stable for a very short time but then has a fold and goes back until about $\delta = 0.57$ where another fold produces the stable 2-year solution that continues up to $\delta = 1$. The two solutions give different singular points, and bistability between the 1- and 2-year solutions causes an overlap for $\delta \in (0.57, 0.63)$ between each branch of singular points, as seen in figure 1(c) from the main text.

Both singular points were found to be CSSs, although for amplitudes within the bistability region, the $T = 2$ singular point can only be reached by evolution from initial transmission coefficient β_0 greater than the lower bound of the bistability region. This is due to the fact that for β_0 less than this point, the population never reaches the period-doubling bifurcation, see figure E.1(b), and so it doesn't switch between the attractors, and hence the host evolves towards the lower singular point with period $T = 1$.

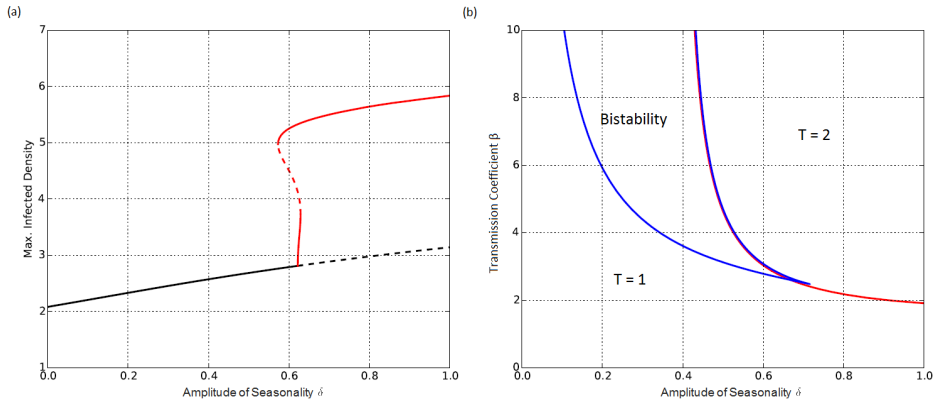

Figure E.1: (a) Stability of solutions to the population equations (1) & (2) in the main text when amplitude δ varies. Black lines - solution with period 1; Red lines - solution with period 2; Solid lines - stable solution; Dashed lines - unstable solution. (b) 2D bifurcation plot of transmission coefficient β vs amplitude δ. Red - period-doubling bifurcation; Blue - fold bifurcations. Both graphs use default parameters with $\hat{a_0} = 104$, $\gamma = 0$ & $\beta = 2.87$ in (a), and were created using AUTO-07p.

F Evolution of hosts with a longer lifespan

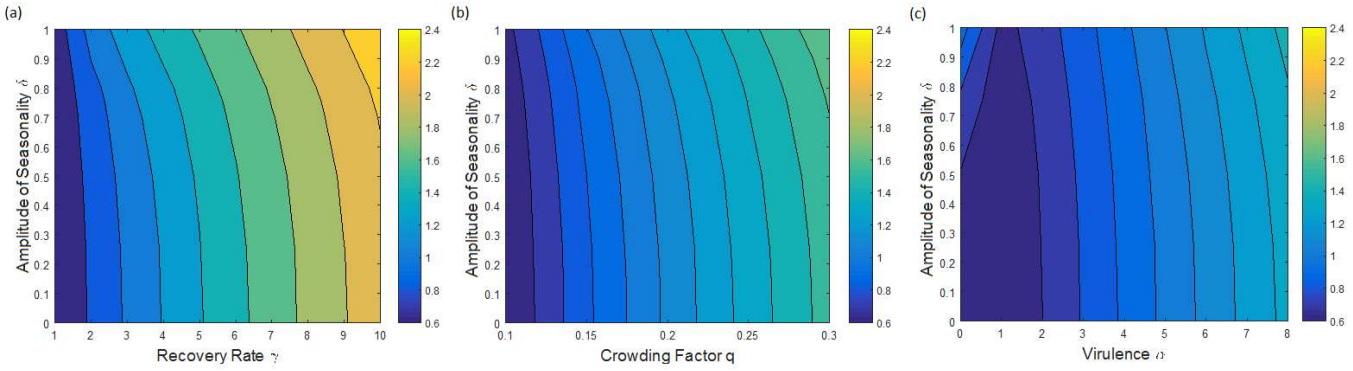

Figure F.1: Two-dimensional contour plots showing the change in the singular point β^* as amplitude δ and (a) recovery rate γ, (b) crowding factor q and (c) virulence α vary. Other parameters were fixed at default values from the main text with $\gamma = 1$ & $b = 0.5$.

In this section we let the parameters take default values with baseline mortality rate decreased to $b = 0.5$ (longer-lived hosts). Figure F.1 shows the CSS singular point β^* for varying amplitude δ with recovery rate γ, crowding factor q and virulence α. In this case, the evolutionary behaviour of the host remains the same for all values of δ and is caused by changes in the average infected population in all three cases. These results are in contrast to those in the main text, where we found that the evolutionary behaviour changes for high amplitudes. Note in particular that the host evolves highest defence for an intermediate virulence for all values of δ as seen elsewhere (van Baalen, 1998), although

the dip is smaller for low amplitudes and so doesn't show up in figure F.1(c). This indicates that the evolution of hosts with a shorter lifespan may be more complicated for high amplitude birth rates, & that high amplitudes has a more significant impact on the populations dynamics for shorter lifespans. However, we can expect the same behaviour for high or low amplitude birth rates for longer-lived hosts.

Literature Cited Only in the Appendix

E. Doedel and B. Oldman. AUTO 07-p: Continuation and bifurcation software for ordinary differential equations. Concordia University. 2009